American Mineralogist, Volume 92, pages 748–752, 2007

Tilt and buckling modes, and acoustic anisotropy in layers with post-perovskite connectivity

Ian P. Swainson* and André L. Yonkeu

Canadian Neutron Beam Centre, National Research Council of Canada, Station 18, Chalk River Laboratories, Chalk River, Ontario, K0J 1J0, Canada

Abstract

The effect of the anisotropic connectivity within the layers of the post-perovskite, $CaIrO_3$, structure are examined using a Rigid Unit Mode and group theory approach, and possible commensurate tilt structures are given. It is shown that the anisotropic bonding of the sheet may give rise to preferred directions of buckling for such structures and anisotropy in the speed of sound.

Keywords: Post-perovskite, $CaIrO_3$, tilt modes, layer structures, buckling modes, acoustic anisotropy

Introduction

In the Earth's mantle, the mineral perovskite, $MgSiO_3$, is a dominant phase over a great range of (*P*, *T*). The perovskite structure is a fully three-dimensionally corner-bonded framework (Mitchell 2002). The highest possible symmetry of such a framework is cubic $Pm\bar{3}m$, in which the Si, at the centers-of-mass of the octahedra, sit on the corners of the cubic unit cell, and all the O atoms, at the corners of the octahedra, lie along the edges of the unit cell, halfway between each Si atom (Mitchell 2002; Howard and Stokes 1998, 2002; Glazer 1972, 1975). $MgSiO_3$ perovskite crystallizes in an orthorhombic subgroup, *Pnma*, related to the $Pm\bar{3}m$ group by rotation or tilting of octahedra (Glazer 1972, 1975; Howard and Stokes 1998, 2002).

A phase transition from the framework structure of $MgSiO_3$ perovskite to the structure of what has become known as post-perovskite (Fig. 1) has been shown both experimentally and by simulation to occur at pressures in excess of 120 GPa (Iitaka et al. 2004; Oganov et al. 2004; Murakami et al. 2004; Ono et al. 2006). The post-perovskite structure is usually described as a layer structure with $BX_{6/2}$ octahedra corner-connected along **c**, vertically edge bonded along **a**, stacked in layers along **b**, separated by a spacer layer of AX_8 trigonal bicapped prisms (Mitchell et al. 2004). Recently, a family of intermediate slip structures between perovskite and post-perovskite has been proposed (Oganov et al. 2005). The operation of a plastic shear deformation may be at the origin of the observed orientation of the anisotropy of the speed of sound in the D'' layer (Iitaka 2004; Oganov and Ono 2004; Oganov et al. 2005).

The post-perovskite structure is shared by several inorganic solids at ambient pressures such as $CaIrO_3$, $UFeS_3$, $UMnS_3$, $UScS_3$ (Narducci et al. 1998), $UMnSe_3$, $ThMnSe_3$ (Iijjali et al. 2004), and LnYbQ_3 (Ln = La, Ce, Pr, Nd, Sm), Q = (S, Se) (Mitchell et al. 2004), some of which can also crystallize in the *Pnma* perovskite framework. It is likely that further compounds will be found to crystallize into layers with this connectivity at low or ambient pressures. The increased mineralogical and seismological interest in post-perovskite will probably instill a greater interest in such structures.

Tilt instabilities in frameworks of corner-linked octahedra have been a source of research interest for several decades. These include the ABX_3 true perovskite structures (Glazer 1972, 1975; Howard and Stokes 1998, 2002), and the corner-bonded perovskite-like layer structures ABX_4 (Deblieck 1986; Deblieck et al. 1985) and A_2BX_4 (Hatch and Stokes 1985, 1987, 1989). In these two layer structures, the octahedra share four out of their six corners by being bonded within the layer, leaving two unconnected corners projecting out of the layer. The latter corners are unimportant to the mechanical behavior of the layer, so the instabilities in these systems can be approximated to those of a layer of rigid corner-connected squares, where there is a potential instability at every wavevector (Swainson 2005).

In a layer composed not of discrete particles, but of rigid octahedra, a transverse acoustic mode generates a rotational couple on the octahedra, in addition to a translation (Nye 1985). If there is no angular term governing the mutual orientation of the octahedra, such modes with wavevectors lying in the plane will have zero frequency. Figure 2 shows that where the wavelength of such buckling modes happens to be equal to twice the spacing between neighboring octahedra, the centers of mass of the octahedra sit on nodes and the displacement eigenvectors are a pure rotation of the octahedra, i.e., a tilt mode (Swainson 2005). As λ increases, ($k \rightarrow 0$), the displacement eigenvectors take on an increasing component of rigid body displacement normal to the layer.

Edge connectivity increases the density compared to a purely corner-connected structure, but it also reduces flexibility. The tilting seen in $CaIrO_3$ increases the density of packing further by shortening the spacing along the corner-connected **c** direction. The connecting edges run vertically, sticking slightly above and slightly below the plane defined by the centers of mass of the octahedra.

This study examines the effect of vertical edge connectivity on the mechanical instabilities of a $BX_{6/2}$ layer, the possible tilt and buckling instabilities in such a layer, and the acoustic anisotropy that might be expected from uncoupled layers of rigid $BX_{6/2}$

* E-mail: ian.swainson@nrc.gc.ca

0003-004X/07/0506–748$05.00/DOI: 10.2138/am.2007.2456

octahedra in the familiar $CaIrO_3$ tilt system. Given the interest in compounds with this structure that are analogous to the $MgSiO_3$ post-perovskite phase, we also list the simple tilt structures that are likely candidates to be found from phase transitions within this structure type. The intermediate slip structures between the three-dimensional perovskite framework and post-perovskite layer system (Oganov et al. 2005) would also possess tilt structures, although we do not examine these here.

Direct space view of allowed tilts

Post-perovskite can be described as formed of **a**-axis columns of vertically edge-bonded octahedra that are connected into a layer by their corners along **c**. For edge-bonded columns the rotation of an octahedron about the column axis requires all octahedra to rotate in phase (Fig. 3a). The familiar post-perovskite structure possesses tilting of these columns about **a**, which we denote θ_x. A view down **b**, perpendicular to an untilted layer, shows the second type of allowed tilting (Fig. 3b), those about the unshared edges of the octahedra that lie perpendicular to **b**, and which we label θ_y; as the shared edges that fuse the octahedra into columns are parallel to the layer axis, **b**, the vertical edge connectivity provides no more constraint than corner-connectivity for θ_y-rotations. The resulting pattern of θ_y-tilts in the (010) plane is identical to one from the fully corner-connected layers (Hatch and Stokes 1985, 1987, 1989; Deblieck 1986; Deblieck et al. 1985).

Calculations

Two approaches are used in this study. The first is a phonon method calculating the Rigid Unit Mode (RUM) spectrum (Dove et al. 1991; Giddy et al. 1993; Hammonds and Dove 1994). The computational program CRUSH implements this by modeling a system in which an isolated octahedron can be visualized as being fused into the network of interest. Each octahedron retains all its corner atoms, and the fusing is done mathematically by giving shared corner atoms the same coordinates, and placing a large spring constant between them. Modes that do not require distortion of these octahedra have zero frequency in this approximation, since no force acts on the spring. The zero-frequency modes may be pure rotational modes (tilts), or they may also possess components of translation of the center-of-mass of the octahedra, such as the buckling instabilities in the layer.

The existence of RUMs in a solid is due to the existence of a few extra degrees of freedom. The constraints, partly counteracting the degrees of freedom, are the interconnections between polyhedra [i.e., the shared corners and edges (Dove et al. 1991; Hammonds et al. 1998a, 1998b)]. Layers with post-perovskite-connectivity, with both vertical edge and corner connectivity, are expected to be less flexible than fully corner-connected ABX_4 and A_2BX_4 perovskite-like layer structures, but more flexible than a rigid slab.

The second method of analysis is based on group theory and follows that developed by Hatch and Stokes (1985, 1987, 1989), who first applied it to the study of tilts in the A_2BX_4 perovskite-like layer structures. The group theory codes used in this study were ISOTROPY (Stokes and Hatch 2002) and ISODISPLACE (Campbell et al. 2006). Points of high symmetry in the Brillouin Zone (BZ) are examined for irreducible representations that transform as pure rotations about the centers of mass of the octahedra. Only a few of the candidate representations yield patterns of rotations that respect the connectivity of the network, without requiring strong distortion. These are the allowed tilt modes.

The eigenvectors of the RUMs from CRUSH calculations at high symmetry points in the BZ are then examined and compared to the patterns of pure rotations of octahedra and pure translations described by the irreducible representations at these points. This enables us to label the irreducible representation associated with a RUM.

For the purposes of the group descriptions an untilted model was constructed in *Cmmm* with the *B* ion sitting on the 2a sites, the corner-connected *X* atom on 2d sites 0, 0, 1/2 and the edge-connected *X* atom on the 4i sites 1/2, *y*, 0. The labeling of the irreducible representations is that of Miller and Love (1967).

The distribution of RUMs in the Brillouin Zone

Cmmm untilted layers

The symmetry of the untilted "aristotype" of post-perovskite-connectivity is *Cmmm* with the lattice spacing *c* being approximately half that of the tilted phase. Figure 4a shows the distribution of RUMs for such layers. The instabilities at *R* correspond to θ_y tilts, while those at *T* and *Z* correspond to θ_x tilts.

A common feature of decoupled layers stacked in an orthorhombic cell perpendicular to the **b**-axis, are three lines of soft modes sharing wavevectors from Γ-*Y* representing the translations of the layers along the three orthogonal directions, T_x, T_y, and T_z. These exist for rigid slabs. The post-perovskite layer connectivity has additional degrees of freedom (Fig. 3). An untilted layer is soft to transverse acoustic modes with $\mathbf{k} = (0, 0, \zeta)$ containing a component of translation normal to the layer, T_y. (Longitudinal acoustic modes with $\mathbf{k} = (0, 0, \zeta)$, and T_z displacements are of high frequency as the hinges are collinear in *c* and the octahedra are rigid.) The vertical edge connectivity requires all octahedra to rotate in phase in columns along *a* for θ_x-style couples, so that a single plane of buckling modes $\mathbf{k} = (0, \xi, \zeta)$ link the pure rotations of the columns, θ_x, at $(0, \xi, 1/2)$ to the Γ-point mode of symmetry, Γ_4^-, which transforms as T_y.

In other words, in contrast to rigid slabs, zero-frequency modes that contain components of T_y displacements are now spread into an entire plane, rather than restricted to a single line of wavevectors. Nevertheless, in comparison to the distribution of buckling modes in an isolated corner-bonded layer, where they fill the entire volume of the BZ (Swainson 2005), the distribution in post-perovskite layers is sharply restricted.

Cmcm $CaIrO_3$ tilt system

The $CaIrO_3$ tilt system is related to the *Cmmm* parent by the Z_3^+ representation (Fig 1). The tilt and buckling instabilities are modified once the $CaIrO_3$ tilt structure is adopted (Fig. 4b). As the **c**-axis is doubled with respect to the untilted layer, the single remnant line of θ_y tilts, which ran along $(\frac{1}{2}, \xi, \frac{1}{2})$ in the untilted form, is now found at $(\frac{1}{2}, \xi, 0)$ passing through the *S* points.

There are two main differences with respect to the untilted layer. First, while a single $(0, \xi, \zeta)$ plane of soft RUM wavevectors persists, there are no pure tilts along the line linking *T* and *Z*, as the θ_x rotational freedom has been already "frozen-in" during the *Cmmm* → *Cmcm* transition. Second, there are now two buckling modes per wavevector in $(0, \xi, \zeta)$. As the corner hinges are no longer collinear in **c** the tilted layer is soft to any acoustics that can also form a θ_x couple (Fig. 3). Therefore, modes with **k** lying in $(0, \xi, \zeta)$ and displacements containing components T_y or T_z have zero frequency (i.e., in contrast to rigid slabs, the only soft acoustic modes restricted to the Γ-*Y* line of wavevectors are those containing T_x displacements).

Symmetry analysis of commensurate pure tilt structures

Table 1 shows the possible simple tilt systems that can result from the tilt modes in the Brillouin Zone shown in Figure 4. The R_2^+ tilt mode is two-dimensional. The order parameter directions

(Campbell et al. 2006) for this representation correspond to the amplitude of tilting of the two layers, related by the *C*-centering, in the structure. For instance, R_2^+ (a, a) corresponds to θ_y-tilting of the two layers with equal amplitudes, whereas R_2^+ (a, b) corresponds to different amplitudes of θ_y-tilt for the two layers. It is possible to combine the θ_y and θ_x tilts in various manners and these are listed as the various possible subgroups of $R_2^+ \oplus Z_3^+$ and $R_2^+ \oplus T_3^+$.

From the data in Table 1, a 4 × 4 matrix may be formed from the rows listed under the basis and the origin shift, by adding a right hand column of [0, 0, 0, 1]. The inverse transpose of this may be used to transform the fractional coordinates into the new phases; e.g., to transform from *Cmmm* to *Fmmm*:

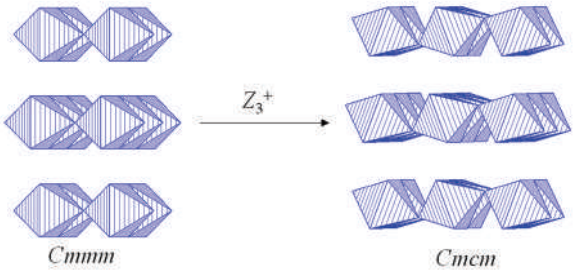

FIGURE 1. The $CaIrO_3$ structure (right) and the untilted parent *Cmmm* phase (left) viewed down a direction near the **a**-axis. The cations are excluded to clarify the relationship between the tilted and untilted layers. Columns of edge-bonded octahedra are corner-bonded along *c* to form a layer, and the octahedra are antiferro-tilted along the column connections. The layers are stacked up the **b**-axis. The label Z_3^+ refers to the representation governing the tilt relating the two structures.

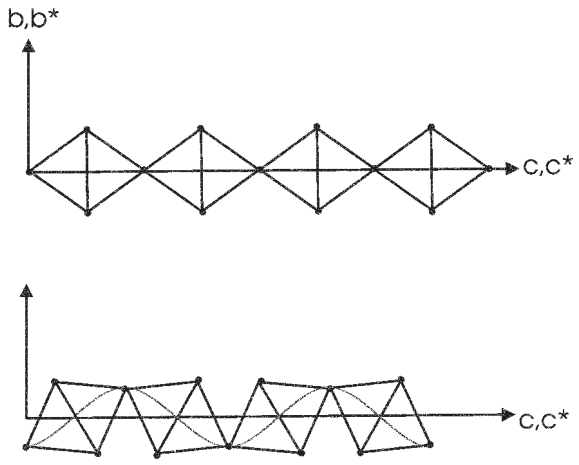

FIGURE 2. The action of a transverse acoustic wave with displacements along *y,* parallel to the layer axis, associated with a transverse acoustic with wavevector **k** = (0,0,ζ). Generally, the displacement can be broken into a rigid body translation, T_y, and a rigid body rotation of the octahedra about the orthogonal **a**-axis, θ_x, normal to the page. For wavelengths of twice the separation of the octahedra (bottom of figure), the centers of mass sit on nodes and the mode becomes a pure θ_x tilt.

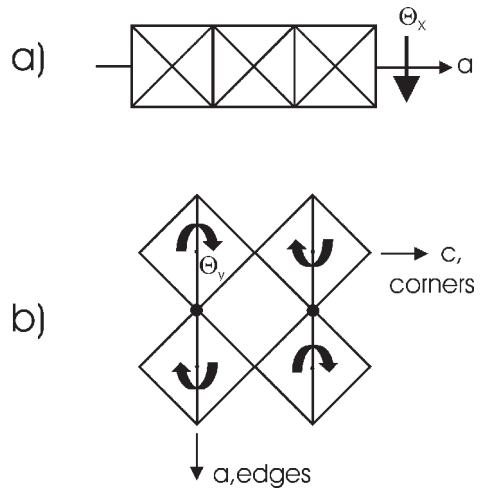

FIGURE 3. (**a**) A rotation of a vertically edge-bonded column of octahedra about the chain axis, θ_x, forces all octahedra in that column to rotate in phase. (**b**) A view normal to an untilted layer, **b**. The vertical edge connection is perpendicular to the paper and is represented with a solid dot. Rotation of one octahedron about this axis, θ_y, causes the pattern of rotations shown that is identical to the pattern observed in corner-bonded layers (i.e., in this projection the vertical edge bonding imposes no more constraint than does corner bonding).

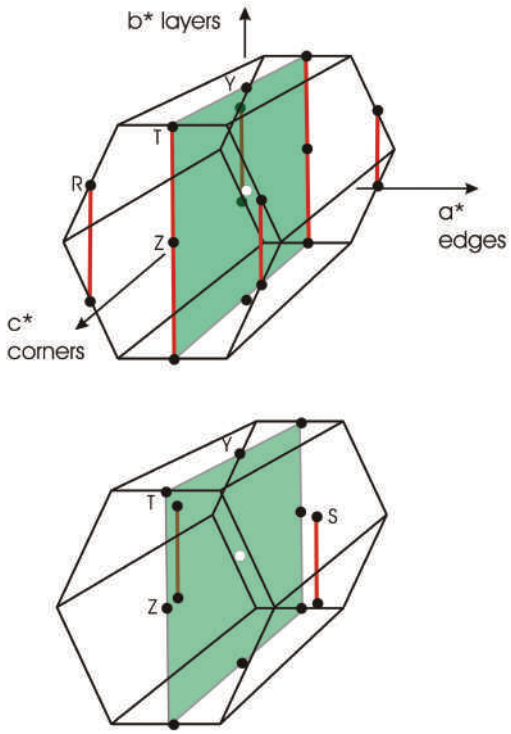

FIGURE 4. The distribution of buckling and tilt modes (excess modes over rigid slabs) of an (**a**) untilted layer (**b**) a layer in the $CaIrO_3$ tilt system plotted in the BZ of the *C*-centered lattice. The red lines are tilts and the green plane represents buckling modes. The white dot gives the location of the Γ-point.

TABLE 1. Subgroups resulting from the action of simple tilt transitions from a *Cmmm* untilted ABX_3 parent where the *B* ion sits on the 2a sites, the corner-connected *X* atom on 2d sites 0, 0, 1/2 and the edge-connected *X* atoms on the 4i sites 1/2, *y*, 0

Rep.	Direction*	Tilt	Subgroup	Basis†	Origin
Z_3^+	(a)	θ_x	*Cmcm*	(1,0,0), (0,1,0), (0,0,2)	(0,0,0)
T_3^+	(a)	θ_x	*Imma*	(−1,0,0), (0,0,2), (0,1,0)	(0,0,0)
R_2^+	(a, 0)	θ_y	*Fmmm*	(2,0,0), (0,2,0), (0,0,2)	(0,½,½)
R_2^+	(a, a)	θ_y	*C2/m*	(−1,1,0), (0,2,0), (½,½,0)	(0,½,½)
R_2^+	(a, b)	θ_y	*C2/m*	(−2,0,0), (0,2,0), (1,1,0)	(½,0,½)
$R_2^+ \oplus Z_3^+$ $R_2^+ \oplus T_3^+$	(a, 0, b)	θ_y, θ_x	*Cmcm*	(2,0,0), (0,2,0), (0,0,2)	(0,0,0)
$R_2^+ \oplus Z_3^+$	(a, a, b)	θ_y, θ_x	$P2_1/m$	(−1,1,0), (0,0,2), (½,½,0)	(0,0,0)
$R_2^+ \oplus T_3^+$	(a, a, b)	θ_y, θ_x	*C2/m*	(−1,1,0), (0,0,2), (−1,−1,0)	(¼,¾,½)
$R_2^+ \oplus Z_3^+$ $R_2^+ \oplus T_3^+$	(a, b, c)	θ_y, θ_x	$P2_1/m$	(−1,1,0), (0,0,2), (1,1,0)	(0,0,0)

Notes: The labeling of representations is that of Miller and Love (1967), and the cell setting is the default of ISOTROPY (Stokes and Hatch 2002).
* The order parameter direction is given to specify the particular distortion for multidimensional representations (Stokes and Hatch 2002).
† The basis gives the axes of the subgroup unit cell with respect to that of the *Cmmm* parent group.

$$\begin{pmatrix} x \\ y \\ z \\ 1 \end{pmatrix}_{Fmmm} = \left[\begin{pmatrix} 2 & 0 & 0 & 0 \\ 0 & 2 & 0 & 0 \\ 0 & 0 & 2 & 0 \\ 0 & \frac{1}{2} & \frac{1}{2} & 1 \end{pmatrix}^{-1} \right]^T \begin{pmatrix} x \\ y \\ z \\ 1 \end{pmatrix}_{Cmmm} .$$

Elastic anisotropy of a single layer

The anisotropic speed of sound distribution in the D" layer has been explained as due to the anisotropic structure of post-perovskite, combined with a preferred orientation of its lattice (Iitaka 2004; Oganov and Ono 2004; Tsuchiya et al. 2004; Oganov et al. 2005). Here we examine the elastic anisotropy an idealized single layer. The dynamical matrix, M, for acoustic phonons with wavevectors in $\mathbf{k} = (0, \xi, \zeta)$ and small $|\mathbf{k}|$ in an orthorhombic lattice has the form (Nye 1985; Dove 1993):

$$\mathrm{M} = \begin{pmatrix} c_{66}\xi^2 + c_{55}\zeta^2 & 0 & 0 \\ 0 & c_{22}\xi^2 + c_{44}\zeta^2 & (c_{23} + c_{44})\xi\zeta \\ 0 & (c_{23} + c_{44})\xi\zeta & c_{44}\xi^2 + c_{33}\zeta^2 \end{pmatrix} .$$

Layered materials frequently show weak interactions between the layers, and this is often an expectation of the elastic behavior of a layer structure. The line of acoustic modes with $\mathbf{k} = (0, \xi, 0)$, and displacements $\mathbf{u} = T_x$, T_y, and T_z have zero frequency for all ξ, so that $c_{66} = c_{22} = c_{44} = 0$, which as we have discussed would also be true of rigid slabs. Isolated planes are unstable in three-dimensions, and for an orthorhombic lattice, $c_{44} = 0$ and $c_{66} = 0$ are two classical elastic instabilities (Terhune et al. 1984). For a layer with internal freedom, there are additional soft elastic constants. In the RUM, approximation of a $CaIrO_3$-tilted layer $c_{22} = c_{33} = c_{23} = c_{44} = c_{66} = 0$.

DISCUSSION

Group theory only gives lists of possible phases, and does not infer preference for any one over another. Some tilt systems may be more common than others, and preference for one tilt structure over another in the perovskite system can be explained from concepts such as ionic radii ratios and the degree of ionic or covalent character of the bonding (Woodward 1997). The order parameter $R_2^+(a, 0)$ and its admixtures with Z_3^+ and T_3^+ are perhaps less likely than others, since physically this would correspond to θ_y tilting of one layer and not the neighboring layers. If such θ_y-tilting of one layer is favored due to interactions with the *A* cations, then it seems likely that the neighboring layers would also have a finite θ_y-tilt. We also deliberately exclude the mixture of T_3^+ and Z_3^+ from Table 1, since this would correspond to complex mixtures of in-phase and out-of-phase θ_x tilting across layers.

We might expect that the plane of buckling modes provide soft modes to incommensurate structures. It is two remnant planes of buckling modes in a tilted A_2BX_4 layer that govern the complex commensurately and incommensurately modulated phases seen in the propylammonium tetrahalometallates (Swainson 2005). This plane of buckling modes is also a potential source of diffuse scattering in diffraction studies of these compounds.

Density functional theory (DFT) static lattice relaxations give exact solutions for ordered structures, but do not always give an understanding of the origin of the calculated values of properties such as elastic constants in terms of a simple model. In contrast to the RUM calculations, the real values of the elastic constants are finite and vary with composition and (*P*, *T*). The only compound with this connectivity whose elastic constants have been studied to date is that of $MgSiO_3$ (Iitaka et al. 2004; Oganov and Ono 2004; Tsuchiya et al. 2004), for which DFT relaxations at $P = 0$ GPa show that c_{22} and c_{33} are smaller than c_{11}, and c_{44} and c_{66} are smaller than c_{55} (Tsuchiya et al. 2004), in reasonable agreement with the approximations of this model. However, c_{23} is larger than c_{12} and c_{13} suggesting that some of the flexibility of the real structure is reduced compared to the ideal RUM calculations. For the many compounds with post-perovskite connectivity that occur at lower or even ambient pressures, the approximation of the structure to a layer with some internal freedom may be a reasonable mechanical description.

ACKNOWLEDGMENTS

We thank M.T. Dove and A. Goodwin (Cambridge U.), and H.T. Stokes and B.J. Campbell (Brigham Young U.) for provision of the codes CRUSH, ISOTROPY, and ISODISPLACE.

REFERENCES CITED

Campbell, B.J., Stokes, H.T., Tanner, D.E., and Hatch, D.M. (2006) ISODISPLACE: a web-based tool for exploring structural distortions. Journal of Applied Crystallography, 39, 607–614.

Deblieck, R. (1986) Group analysis of octahedral librations involved in phonon-induced displacive phase transition in perovskite-related ABX_4 compounds. Acta Crystallographica, A42, 318–325.

Deblieck, R., Van Tendeloo, G., Van Landuyt, J., and Amelinckx, S. (1985) A structure classification of symmetry-related perovskite-like ABX_4 phases. Acta Crystallographica, B41, 319–329.

Dove, M.T. (1993) An introduction to lattice dynamics. Cambridge University Press, U.K.

Dove, M.T., Giddy, A.P., and Heine, V. (1991) Rigid unit model of displacive phase transitions in silicates. Transactions of the American Crystallographic Association, 27, 65–74.

Giddy, A.P., Dove, M.T., Pawley, G.S., and Heine, V. (1993) The determination of rigid unit modes as potential soft modes for displacive phase transitions in framework crystal structures. Acta Crystallographica, A49, 697–703.

Glazer, A.M. (1972) The classification of tilted octahedral in perovskites. Acta Crystallographica, B28, 3384–3392.

——— (1975) Simple ways of determining perovskite structures. Acta Crystallographica, A31, 756–762.

Hammonds, K.D. and Dove, M.T. (1994) CRUSH—a FORTRAN program for the analysis of the rigid-unit mode spectrum of a framework silicate. American Mineralogist, 79, 1207–1209.

Hammonds, K.D., Bosenick, A., Dove, M.T., and Heine, V. (1998a) Rigid unit modes in crystal structures with octahedrally coordinated atoms. American Mineralogist, 83, 476–479.

Hammonds, K.D., Heine, V., and Dove, M.T. (1998b) Rigid unit modes and the quantitative determination of the flexibility possessed by zeolite frameworks. Journal of Physical Chemistry B, 102, 1759–1767.

Hatch, D.M. and Stokes, H.T. (1985) Practical algorithm for identifying subgroups of space groups. Physical Review, B31, 2908–2912.

——— (1987) Classification of octahedral tilting phases in the perovskitelike A_2BX_4 structure. Physical Review, B35, 8509–8516.

——— (1989) Phase transitions in the perovskitelike A_2BX_4 structure. Physical Review, B39, 9282–9288.

Howard, C.J. and Stokes, H.T. (1998) Group Theoretical Analysis of Octahedral Tilting in Perovskites. Acta Crystallographica, B54, 782–789.

——— (2002) Group-theoretical analysis of octahedral tilting in perovskites. Erratum. Acta Crystallographica, B54, 565.

Iijjali, I., Mitchell, K., Fu, Q.H., and Ibers, J.A. (2004) Syntheses and characterization of the actinide manganese selenides $ThMnSe_3$ and $UMnSe_3$. Journal of Solid State Chemistry, 177, 257–261.

Iitaka, T., Hirose, K., Kawamura, K., and Murakami, M. (2004) The elasticity of the $MgSiO_3$ post-perovskite phase in the Earth's lowermost mantle. Nature, 430, 442–445.

Miller, S.C. and Love, W.F. (1967) Irreducible representations of space groups and co-representations of magnetic space groups. Pruett Press, Boulder, Colorado.

Mitchell, K., Somers, R.C., Fu, Q.H., and Ibers, J.A. (2004) Syntheses, structure and magnetic properties of several $LnYbQ_3$ chalogenides, Q = S, Se. Journal of Solid State Chemistry, 177, 709–713.

Mitchell, R.H. (2002) Perovskites: Modern and ancient. Almaz Press, Thunder Bay, Ontario.

Murakami, M., Hirose, K., Kawamura, K., Sata, N., and Ohishi, Y. (2004) Post-perovskite phase transition in $MgSiO_3$. Science, 304, 855–858.

Narducci, A.A. and Ibers, J.A. (1998) Ternary and Quaternary Uranium and Thorium Chalcogenides. Chemistry of Materials, 10, 2811–2823.

Oganov, A.R. and Ono, S. (2004) Theoretical and experimental evidence for a post-perovskite phase of $MgSiO_3$ in Earth's D" layer. Nature, 430, 445–448.

Oganov, A.R., Martonak, R., Laio, A., Raiteri, P., and Parrinello, M. (2005) Anisotropy of Earth's D'' layer and stacking faults in the $MgSiO_3$ post-perovskite phase. Nature, 438, 1142–1144.

Ono, S., Kikegawa, T., and Ohishi, Y. (2006) Equation of state of $CaIrO_3$-type $MgSiO_3$ up to 144 GPa. American Mineralogist, 91, 475–478.

Nye, J.F. (1985) Physical properties of crystals: Their representation by tensors and matrices. Oxford University Press, U.K.

Stokes, H.T. and Hatch, D.M. (2002) ISOTROPY 6.4.2. Physics Department, Brigham-Young University, Utah (http://stokes.byu.edu/isotropy.html).

Swainson, I.P. (2005) Tilt and acoustic instabilities in ABX_4, A_2BX_4 and ABX_3 perovskite structure types: their role in the incommensurate phases of the organic-inorganic perovskites. Acta Crystallographica, B61, 616–626.

Terhune, R.W., Kushida, T., and Ford, G.W. (1984) Soft acoustic modes in trigonal crystals. Physical. Review B, 32, 8416–8418.

Tsuchiya, T., Tsuchiya, J., Umemoto, K., and Wentzcovitch, R.M. (2004) Elasticity of post-perovskite $MgSiO_3$. Geophysical Research Letters, 31, L14603.

Woodward, P.M. (1997) Octahedral tilting in perovskites: II Structure stabilizing forces. Acta Crystallographica, B53, 44–66.

MANUSCRIPT RECEIVED SEPTEMBER 20, 2006
MANUSCRIPT ACCEPTED JANUARY 24, 2007
MANUSCRIPT HANDLED BY ARTEM OGANOV